BULLETIN OF THE CHEMICAL SOCIETY OF JAPAN, VOL. 44, 1800—1807 (1971)

The Photonuclear Reactions Leading to ^{24}Na and ^{28}Mg

Tatsuya SAITO*

Department of Chemistry, Faculty of Science, Tohoku University, Katahira-cho, Sendai

(Received November 24, 1970)

The photonuclear reaction yields of ^{24}Na and ^{28}Mg in magnesium, aluminum, silicon, phosphorus, and sulfur were obtained at energies between 20 MeV and 250 MeV by the induced radioactivity method. The ^{12}C(γ,n)^{11}C yield was used as a standard for the beam monitor. The excitation curves of the ^{27}Al→^{24}Na, ^{28}Si→^{24}Na, ^{30}Si→^{28}Mg, ^{31}P→^{24}Na, ^{31}P→^{28}Mg, ^{32}S→^{24}Na, and ^{32}S→^{28}Mg reactions were obtained from the yields by the photon-difference method. Each of these excitation functions indicates a peak in the 50—70 MeV energy range, except in the case of the sulfur target, in which the peak is due to the contribution from the compound-nucleus process. The interaction of photons with nuclei at photon energies exceeding the peak energy region probably does not lead to the formation of the compound nucleus. In the energy range from 70 MeV up to 150 MeV, the cross sections are due to the contribution from the quasi-deuteron process. At energies above 150 MeV and up to 250 MeV, the quasi-deuteron and pion production processes compete. In the high-energy photonuclear reaction mechanisms, the quasi-deuteron and pion production processes must be considered at the initial cascade process, but the evaporation process may be considered after the cascade process.

Photonuclear reactions have been studied, and detailed information has been obtained in the low-energy giant-resonance region.[1-3] Above the giant-resonance region, however, our information about the photonuclear cross sections and the reaction mechanisms is very scarce.

Many workers have investigated high-energy reactions induced by high-energy-charged particles, and the details of these mechanisms are by now well known.[4] The mechanism of high-energy nuclear reactions, the cascade evaporation process, is currently regarded as providing the proper description for reactions initiated by particles with incident energies large in comparison with the binding energies of the nucleons within the target nucleus.[5,6] A similar reaction induced by high

* Present address: Department of Applied Chemistry, Faculty of Engineering, Tohoku University, Sendai.

1) R. Montalbetti, L. Katz, and J. Goldemberg, *Phys. Rev.*, **91**, 659 (1953).
2) R. Nathans and J. Halpern, *ibid.*, **93**, 437 (1954).
3) B. L. Berman, J. T. Caldwell, R. R. Harvey, M. A. Kelly, R. L. Bramblett, and S. C. Fultz, *ibid.*, **162**, 1096 (1967).
4) J. M. Miller and J. Hudis, *Ann. Rev. Nucl. Sci.*, **9**, 159 (1959).
5) K. Chen, Z. Fraenkel, G. Friedlander, J. R. Grover, J. M. Miller, and Y. Shimamoto, *Phys. Rev.*, **166**, 949 (1968).
6) R. G. Korteling and A. A. Caretto, Jr., *ibid.*, **CI**, 1960 (1970).

energy bremsstrahlung with a maximum energy greater than 100 MeV was expected. It is an interesting problem to study the mechanisms by which the complex nucleus absorbs high-energy photons. In this fields, the following processes have been proposed to explain the photonuclear cross section data: the quasi-deuteron and the pion production processes. In order to explain the high-energy photonuclear reactions, several experiments have previously been reported on the yields and cross sections as determined by the activation method.[7-9] Debs *et al.*[7,8] irradiated several elements of medium weight by 320 MeV bremsstrahlung, thus obtaining the relative yields. By their data, the mechanism of the high-energy photonuclear reaction was explained by a model in which, after a direct process, a few particles were emitted from a struck nucleus by evaporation. Di Napoli *et al.*[10,11] irradiated carbon and iodine at energies between 300 MeV and 1000 MeV, and showed the (γ, n) excitation curves. In this energy region, these reactions result from the photopion process. Van Hise *et al.*[12] irradiated ^{32}S, ^{40}Ca, and ^{66}Zn at energies up to 300 MeV. The reactions in these experiments generally receive important contributions from both the quasi-deuteron and pion emission processes above the pion threshold. The reactions leading to ^{24}Na have already been reported. The excitation curves for the ^{27}Al→^{24}Na and ^{31}P→^{24}Na reactions up to 260 MeV have been reported by Gorbunov *et al.*[13] In addition, the yields of ^{24}Na from the ^{27}Al→^{24}Na, ^{28}Si→^{24}Na, ^{31}P→^{24}Na, ^{32}S→^{24}Na, ^{39}K→^{24}Na, and ^{40}Ca→^{24}Na reactions have been reported at energies from 100 MeV to 1200 MeV by Noga *et al.*[14]

The purpose of the present experiments is to obtain information about the character of the interaction of photons with nuclei in the energy range from 20 MeV to 250 MeV. Especially, the work reported here will improve our understanding of the high-energy photonuclear processes that occur at energies above the low-energy giant-resonance region.

Experimental

Targets and Irradiations. The target elements used in this experiment were magnesium, aluminum, silicon, phosphorus, sulfur, carbon, and gold. All of them were in their elemental form and well sufficiently pure. The impurities in these target substances were found to be negligible in amount. The irradiation sample had a weight of 100—1000 mg and was contained either in a quartz tube or in a Pyrex tube. The experimental methods were described in detail in previous papers.[15-17] The sources of electrons were obtained with the linear electron accelerator of Tohoku University from 30 MeV to 250 MeV and with that of the Japan Atomic Energy Research Institute at 20 MeV. The electron beam in the energy region from 30 MeV to 75 MeV, accelerated by the "High Current" accelerating section of the machine, produced bremsstrahlung in a 3-mm-thick platinum converter.

The sample tubes were held in alignment with the bremsstrahlung beam and were placed in a water-cooled stainless holder.

In the energy region from 100 MeV to 250 MeV, the electron beam accelerated by the "High Energy" accelerating section produced bremsstrahlung in a 0.2-mm-thick tantalum converter. All of these electrons were not converted to bremsstrahlung in a converter. The rest of the electrons were swept away with a sweeping magnet. The sample tubes were held in alignment with the bremsstrahlung beam behind the sweeping magnet and were placed in an aluminum holder.

The electron beam at 20 MeV was converted with a 2-mm-thick platinum converter. The irradiation time was 20 min—2 hr.

Radioactivity Measurement. After irradiation, the target samples were each transferred into "cold" aluminum foils. The gamma-ray spectra were measured at a suitable counting geometry by using a 36-cm^3 Ge(Li) detector coupled to a TMC 1024-channel pulse-height analyzer and a 3″ϕ×3″ NaI(Tl) crystal coupled to a Toshiba 800-channel pulse-height analyzer.

Nuclide identification for ^{24}Na, ^{28}Mg, ^{11}C, and ^{196}Au was made from the knowledge of the target nuclides,[18] the gamma-ray spectra, and the decay data. In these experiments, chemical separation was used if necessary, and gamma-ray spectrometric measurements were performed after having

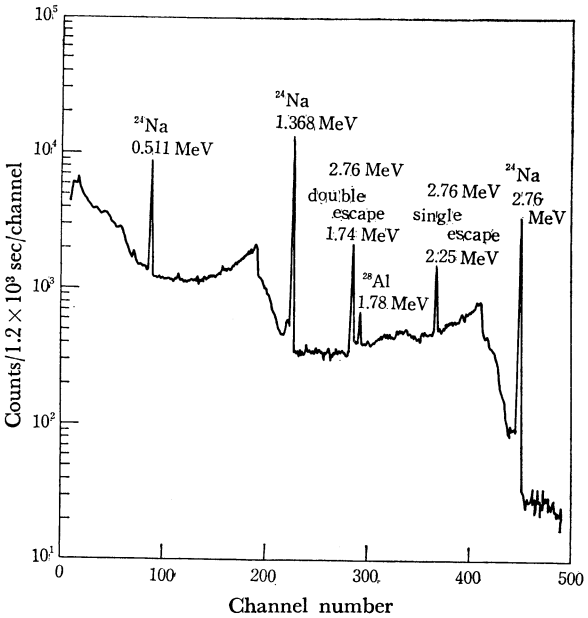

Fig. 1. Gamma-ray spectrum of sulfur target irradiated by 250 MeV bremsstrahlung measured with the 36 cm^3 Ge(Li) detector.

7) R. J. Debs, J. T. Eisinger, A. W. Fairhall, I. Halpern, and H. G. Richter, *ibid.*, **97**, 1325 (1955).
8) I. Halpern, R. J. Debs, J. T. Eisimger, A. W. Fairhall, and H. G. Richter, *ibid.*, **97**, 1327 (1955).
9) T. T. Sugihara and I. Halpern, *ibid.*, **101**, 1768 (1956).
10) V. Di Napoli, F. Dobiti, and F. Salvetti, *Nuovo Cim.*, **48 B**, 1 (1967).
11) V. Di Napoli, F. Dobiti, and F. Salvetti, *ibid.*, **55 B**, 95 (1968)
12) J. R. Van Hise, R. A. Meyer, and J. P. Hummel, *Phys. Rev.*, **139** 554 (1966).
13) A. N. Gorbunov, F. P. Denisov, and V. A. Kolotukhin, *Sov. Phys. JETP*, **11**, 783 (1960).
14) V. I. Noga, Yu. N. Ranyuk, and P. V. Sorokin, *Sov. J. Nucl. Phys.*, **9**, 673 (1969)
15) Y. Oka, T. Kato, K. Nomura, and T. Saito, This Bulletin, **40**, 575 (1966).
16) Y. Oka, T. Kato, K. Nomura, and T. Saito, *J. Nucl. Sci Technol.*, **4**, 346 (1967).
17) Y. Oka, T. Kato, and I. Nagai,. *ibid.*, **4**, 300 (1967)
18) C. M. Lederer, J. M. Hollander, and I. Perlman, "Table of Isotopes," 6th edn., J. Wiley and Sons Inc., New York, London (1968).

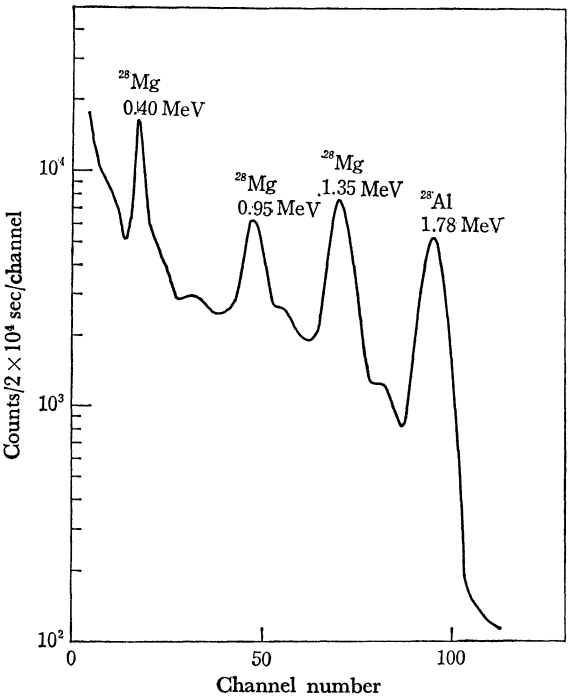

Fig. 2. Gamma-ray spectrum of magnesium fraction from phosphorus irradiated by 200 MeV bremsstrahlung with the 3″ϕ×3″ NaI(Tl) crystal.

been cooled for a time.

Typical gamma ray spectra are shown in Figs. 1 and 2.

Yield Calculation. The disintegration rate was determined by absolute calculations, *i.e.*, the chemical yield, the counting efficiencies, the branching ratio, and the internal conversion ratio. Each of these target samples was wrapped with a thin sheet of gold which was used for the determination of the relative intensity of the bremsstrahlung dose. The intensity integrated over the time of irradiation was standardized by means of the $^{12}C(\gamma,n)^{11}C$ reaction, whose absolute yield had been measured as a function of the peak bremsstrahlung energy up to 260 MeV by Barber *et al.*[19]

The yield was expressed by the following equation:[15]

$$Y(E) = \frac{D_0}{IM(1-e^{-\lambda t})}$$

where D_0 is the disintegration rate at the end of irradiation, I is the radiation dose rate, M is the amount of target nucleus expressed in atoms, and λ is the decay constant. The target elements used were not enriched ones, and it was assumed for the sake of simplicity that each of these elements consisted entirely of its most abundant isotope.

Results

The yield curves for the $^{25}Mg(\gamma, p)^{24}Na$, $^{27}Al\rightarrow{}^{24}Na$, $^{28}Si\rightarrow{}^{24}Na$, $^{31}P\rightarrow{}^{24}Na$, and $^{32}S\rightarrow{}^{24}Na$ reactions and the $^{12}C(\gamma, n)^{11}C$ curve for the monitor reaction are shown in Figs. 3 and 4, while those for the $^{30}Si(\gamma, 2p)^{28}Mg$, $^{31}P(\gamma, 3p)^{28}Mg$, and $^{32}S(\gamma, 4p)^{28}Mg$ reactions are shown in Fig. 5. The solid points in these figures represent the results obtained. The cross section curves for the $^{27}Al\rightarrow{}^{24}Na$, $^{28}Si\rightarrow{}^{24}Na$, $^{31}P\rightarrow{}^{24}Na$, $^{32}S\rightarrow{}^{24}Na$, $^{30}Si(\gamma, 2p)^{28}Mg$, $^{31}P(\gamma, 3p)^{28}Mg$, and $^{32}S(\gamma, 4p)^{28}Mg$ reactions as calculated from the photon-difference method[20] are shown in Figs. 6—12 respectively.

19) W. C. Barber, W. D. George, and D. D. Reagan, *Phys. Rev.*, **98**, 73 (1955).

Discussion

General Considerations. The wavelength of the bombarding particle energies decreases with an increase in the energy, and at energies around approximately 100 MeV it becomes smaller than the mean distance between nucleons in the nucleus, while the time of interaction of the particles with the nucleus is shorter than the characteristic nuclear time.

The characteristics of high-energy particles enable us to obtain information on nuclear characteristics not accessible to other methods. The individual production rates of a photonuclear reaction can be obtained by the measurement of the cross sections.

Investigations of the evidence of the emission of particles with $Z\geqq 2$, carried out by radiochemical methods, are of extreme importance. The particles emitted have specific characteristics. Most of the

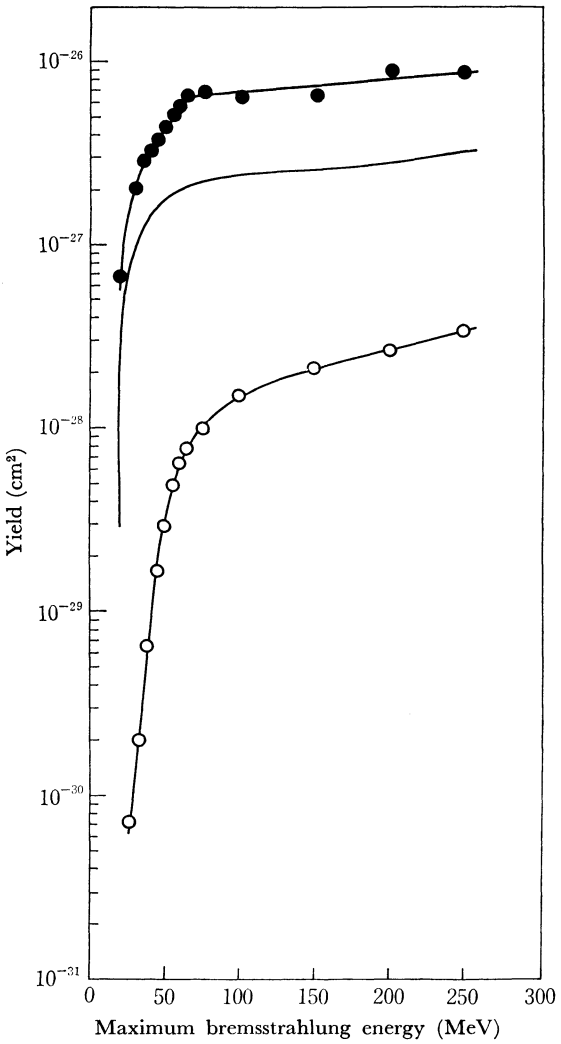

Fig. 3. The yield curves for the reactions $^{25}Mg(\gamma,p)^{24}Na$, $^{27}Al\rightarrow{}^{24}Na$, and $^{12}C(\gamma,n)^{11}C$ as a monitor.
●: $^{25}Mg(\gamma,p)^{24}Na$, ○: $^{27}Al\rightarrow{}^{24}Na$, ——: $^{12}C(\gamma,n)^{11}C$

20) A. S. Penfold and J. E. Leiss, *ibid.*, **114**, 1332 (1959).

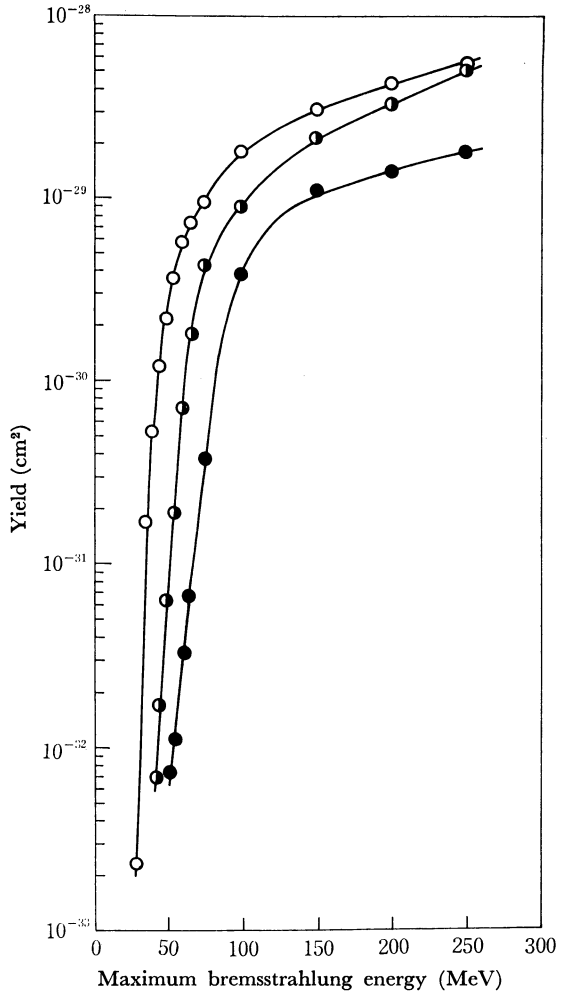

Fig. 4. The yield curves for the reactions ^{28}Si→^{24}Na, ^{31}P→^{24}Na, and ^{32}S→^{24}Na.
○: ^{28}Si→^{24}Na, ◑: ^{31}P→^{24}Na, ●: ^{32}S→^{24}Na

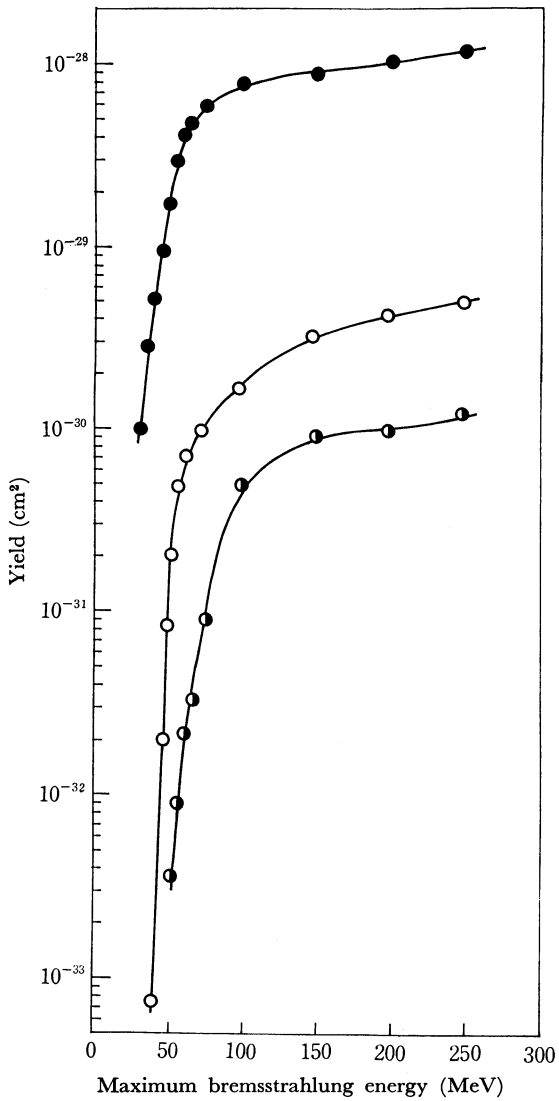

Fig. 5. The yield curves for the reactions ^{30}Si(γ,2p)^{28}Mg, ^{31}P(γ,3p)^{28}Mg, and ^{32}S(γ,4p)^{28}Mg.
●: ^{30}Si(γ,2p)^{28}Mg, ○: ^{31}P(γ,3p)^{28}Mg, ◑: ^{32}S(γ,4p)^{28}Mg

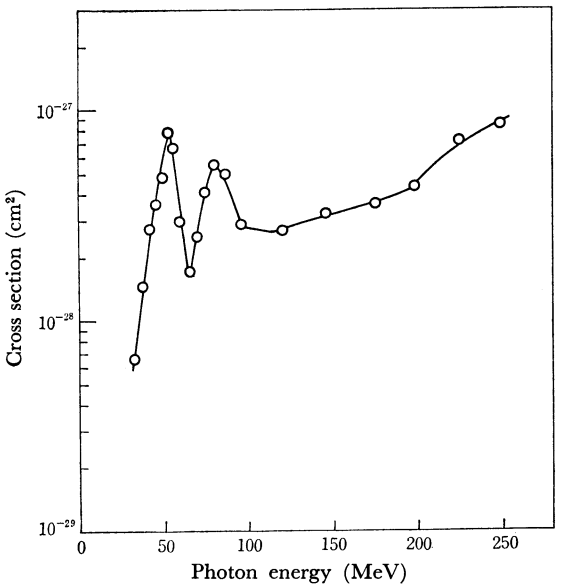

Fig. 6. The excitation function for the reaction ^{27}Al→^{24}Na.

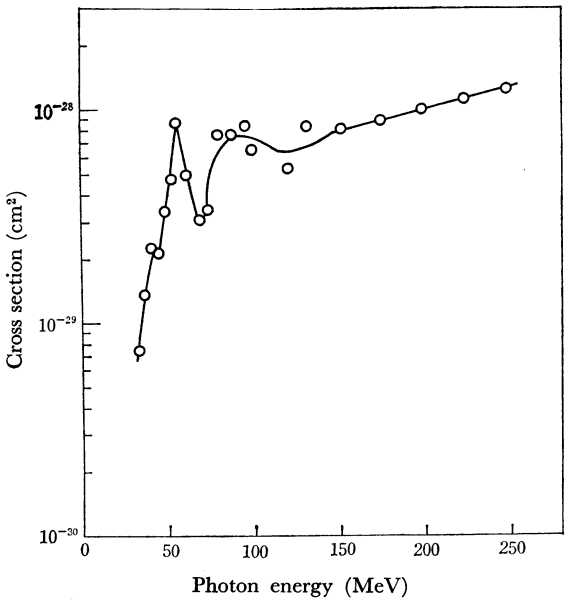

Fig. 7. The excitation function for the reaction ^{28}Si→^{24}Na.

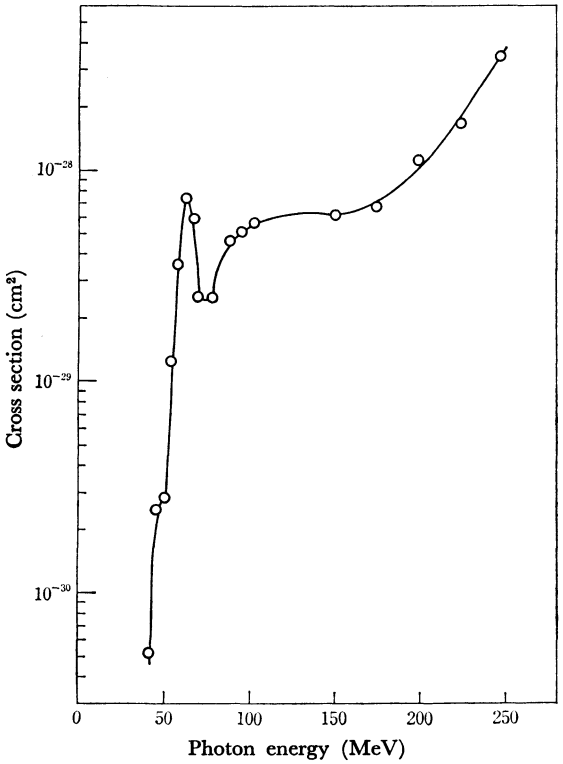

Fig. 8. The excitation function for the reaction $^{31}P \rightarrow {}^{24}Na$.

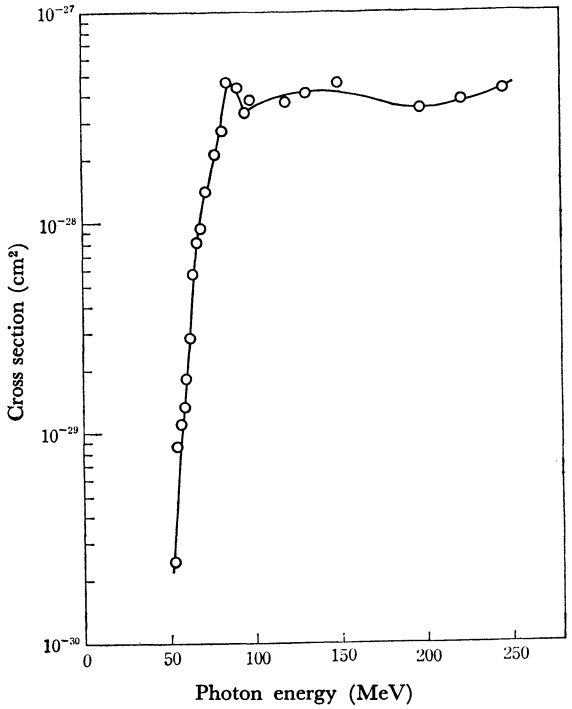

Fig. 9. The excitation function for the reaction $^{32}S \rightarrow {}^{24}Na$.

previous experiments studied high energy photonuclear reactions and involved observations of the emitted nucleons rather than observations of the residual nuclei.

However, the interpretation of a whole series of experimental data obtained in high-energy photonuclear reactions demands an understanding of the structure of the nucleus, especially with regard to the association

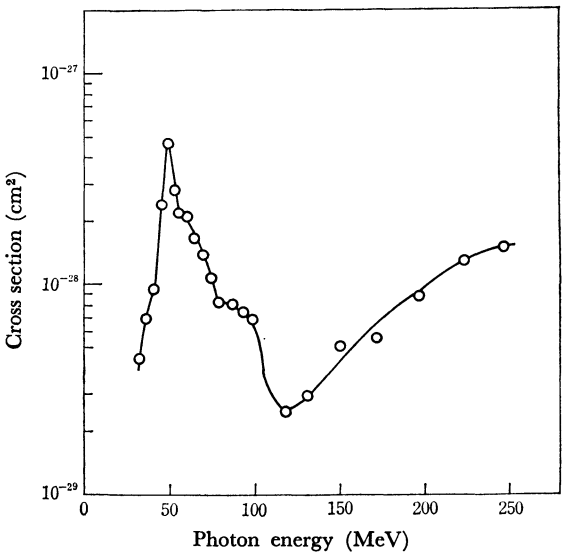

Fig. 10. The excitation function for the reaction $^{30}Si(\gamma,2p)^{28}Mg$.

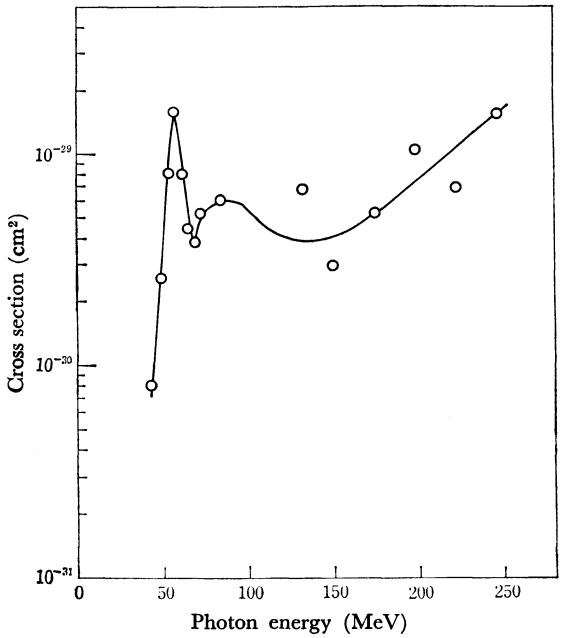

Fig. 11. The excitation function for the reaction $^{31}P(\gamma,3p)^{28}Mg$.

of nucleons within it. The study by the activation method gives important information on the activation yields for the complex nucleus by high-energy photons.

Reaction Path. For convenience in the consideration of the reaction path leading to ^{24}Na and ^{28}Mg, Tables 1 and 2 list the reaction types and the mass threshold values calculated on the basis of the mass differences.[21]

Aluminum and phosphorus are both single isotopic elements, while magnesium, silicon, and sulfur are not.

In the case of the magnesium target, the $Mg \rightarrow {}^{24}Na$ reaction was attributed to the $^{25}Mg(\gamma, p)^{24}Na$ reaction.

21) Nuclidic mass values used were those listed in G. Friedlander, J. W. Kennedy, and J. M. Miller, "Nuclear and Radiochemistry," 2nd ed., J. Wiley and Sons, New York, London (1964), p. 533.

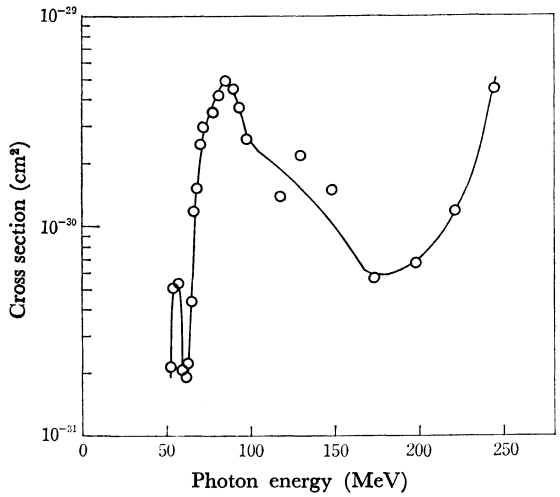

Fig. 12. The excitation function for the reaction ^{32}S(γ,4p)-^{28}Mg.

Table 1. Calculated mass thresholds leading to ^{24}Na

Target nuclide	Abundance (%)	Reaction type	$E_{th}(Q)$(MeV)
^{25}Mg	10.13	(γ, p)	12.06
^{26}Mg	11.17	(γ, pn)	25.94
		(γ, d)	20.93
^{27}Al	100	(γ, 2pn)	31.41
		(γ, dp)	29.20
		(γ, ^{3}He)	23.71
^{28}Si	92.21	(γ, 3pn)	42.99
		(γ, d2p)	40.77
^{29}Si	4.70	(γ, 3p2n)	51.47
		(γ, d2pn)	49.24
		(γ, αp)	23.19
^{30}Si	3.09	(γ, 3p3n)	62.08
		(γ, d2p2n)	59.85
		(γ, αpn)	33.80
^{31}P	100	(γ, 4p3n)	69.36
		(γ, α2pn)	41.17
		(γ, d3p2n)	67.14
		(γ, 3dp)	62.69
		(γ, ^{7}Be)	31.78
^{32}S	95.0	(γ, 5p3n)	78.22
		(γ, α3pn)	49.94
		(γ, d4p2n)	76.00
^{33}S	0.760	(γ, 5p4n)	86.86
		(γ, 2αp)	39.61
		(γ, d4p3n)	84.63
^{34}S	4.22	(γ, 5p5n)	98.27
		(γ, 2αpn)	41.71
		(γ, d4p4n)	96.05
^{36}S	0.014	(γ, 5p7n)	115.13
		(γ, 2αp3n)	58.56
		(γ, d4p6n)	113.84

The ^{27}Al→^{24}Na reaction can result from three different processes, (γ,^{3}He), (γ, dp) and (γ, 2pn), whose thresholds are 23.71, 29.20, and 31.41 MeV respectively. Since the registration of the corresponding activity from the aluminum target began at energies around the thresholds of the (γ, dp) and (γ, 2pn) reactions, it is obvious that, of the three, the latter two processes play the most substantial parts. The ^{27}Al→^{24}Na reaction was attributed to the ^{27}Al(γ, 2pn)^{24}Na reaction by Meyer *et al.*[22]

Table 2. Calculated mass thresholds leading to ^{28}Mg

Target nuclide	Abundance (%)	Reaction type	$E_{th}(-Q)$(MeV)
^{30}Si	3.09	(γ, 2p)	23.99
^{31}P	100	(γ, 3p)	31.27
^{32}S	95.0	(γ, 4p)	40.13
^{33}S	0.760	(γ, 4pn)	48.76
		(γ, d3p)	46.58
^{34}S	4.22	(γ, α2p)	31.91
		(γ, d3pn)	57.96
		(γ, 4p2n)	60.19
^{36}S	0.014	(γ, 2α)	20.48
		(γ, 4d)	68.15
		(γ, 4p4n)	77.04

Sometimes neutron backgrounds are serious enough to cause the production of ^{24}Na by the ^{27}Al(n, α)^{24}Na reaction. Since ^{24}Na activities due to the ^{27}Al(n, α)-^{24}Na reaction irradiated by 20 MeV bremsstrahlung could scarcely be measured, the (n, α) reaction is negligibly small.

The yield of the Si→^{24}Na reaction is the sum of the yields of the ^{28}Si→^{24}Na, ^{29}Si→^{24}Na, and ^{30}Si→^{24}Na reactions. With the excitation energies below 45 MeV, the ^{29}Si(γ, αp)^{24}Na and ^{30}Si(γ, αpn)^{24}Na reactions may play the most substantial part, but above 45 MeV, the yields of the ^{29}Si→^{24}Na and ^{30}Si→^{24}Na reactions are negligibly small, because the isotopic abundances of ^{29}Si and ^{30}Si are as low as 4.70% and 3.09% respectively. Therefore, the reaction product, ^{24}Na, from the ^{28}Si→^{24}Na reaction is obtained *via* the (γ, 3pn) and (γ, d2p) processes. The ^{24}Na yield from ^{31}P is the result of a large number of reactions, of which the energetically most convenient reaction (γ, ^{7}Be) has a threshold of 31.78 MeV, while the energetically least convenient reaction (γ, 4p7n) has a threshold of 69.36 MeV. The experimental threshold of the ^{24}Na yield from ^{31}P is in the neighborhood of 45 MeV. This indicates that, in those reaction processes involving the emission of complex particles, *i.e.*, α-particles, the reaction type (γ, α2pn) plays a substantial part.

The yield of the S→^{24}Na reaction is the sum of the yields of the ^{32}S→^{24}Na, ^{33}S→^{24}Na, ^{34}S→^{24}Na, and ^{36}S→^{24}Na reactions. Below 60 MeV, the ^{34}S(γ, 2αpn)^{24}Na and ^{32}S(γ, α3pn)^{24}Na reactions play the most substantial parts, but above 60 MeV, the ^{32}S(γ, 5p3n)^{24}Na and ^{32}S(γ, α3pn)^{24}Na reactions play the most substantial parts. In order to understand the results of these experiments, the existence of α-particle grouping within the nuclei must be considered.

The reaction paths leading to ^{28}Mg are the ^{30}Si(γ, 2p)^{28}Mg, ^{31}P(γ, 3p)^{28}Mg, and ^{32}S(γ, 4p)^{28}Mg reactions, if the ^{33}S→^{28}Mg, ^{34}S→^{28}Mg, and ^{36}S→^{28}Mg reactions are neglected.

22) R. A. Meyer, W. B. Walters, and J. P. Hummel, *Nucl. Phy.*, **A122**, 606 (1960).

The production yields for ^{24}Na and ^{28}Mg are actually sums of the beta decay chains for their respective masses. The contributions from the products of $Z \neq 11$ to the sodium activites and those of $Z \neq 12$ to the magnesium activities may be disregarded because the ratio of the cross sections for the production of ^{24}Ne and ^{24}Na is negligibly small for proton-induced reactions.[23]

Photonuclear Reaction Yields. In Figs. 3—5 the observed yields data for the reactions studied are plotted as 5 MeV bin width in the energy range between 30 MeV and 65 MeV. In the energy range from 100 MeV to 250 MeV, they were plotted as 50 MeV bin width. In the yield curve, the yield data at 75 MeV bremsstrahlung are added, and they are modified to an adequate smooth curve. The errors in these data are less than 20%. The systematic errors arise from absolute counting factors, beam attenuation in targets, the beam monitor, and the target position monitor. The latter two factors are the main sources of error.

The yield ratios of $Y(^{28}\mathrm{Mg})$ to $Y(^{24}\mathrm{Na})$ were computed for silicon, phosphorus, and sulfur targets, they are shown in Fig. 13.

It should be noted that the yield-ratio curve of silicon does not represent the ratio in a true sense, because not all target nuclides leading to ^{24}Na and ^{28}Mg are the same. In the case of silicon, the rapid decrease up to 45 MeV of the yield ratio curve is due to the differences in the threshold energies, *i.e.* 42.99 MeV and 40.77 MeV leading to ^{24}Na and 23.99 MeV leading to ^{28}Mg. In the energy region between 45 MeV and 250 MeV, the gradual decrease in the yield ratio is independent of the difference in the threshold energy. In the peak energy region, it may be considered that the contribution of the compound nucleus process decreases, while that of the quasi-deuteron process increases.

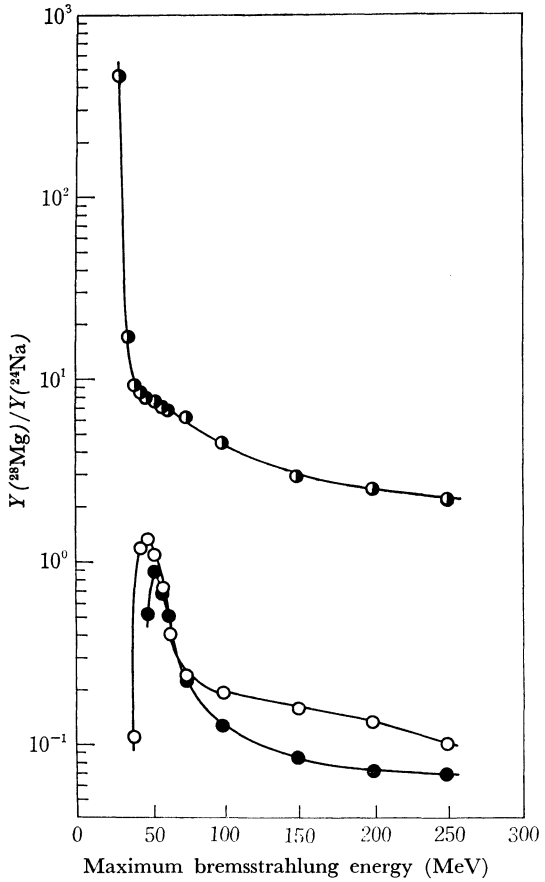

Fig. 13. Yield ratios *versus* maximum bremsstrahlung energy.
◑: $Y(^{30}\mathrm{Si}(\gamma,2\mathrm{p})\ ^{28}\mathrm{Mg})/Y(^{28}\mathrm{Si}\rightarrow^{24}\mathrm{Na})$
○: $Y(^{31}\mathrm{P}(\gamma,3\mathrm{p})\ ^{28}\mathrm{Mg})/Y(^{31}\mathrm{P}\rightarrow^{24}\mathrm{Na})$
●: $Y(^{32}\mathrm{S}(\gamma,4\mathrm{p})\ ^{28}\mathrm{Mg})/Y(^{32}\mathrm{S}\rightarrow^{24}\mathrm{Na})$

Photonuclear Reaction Cross Sections. In Figs. 6—8, 10, and 11, the low energy peak is shown for each figure. In order to explain this, the compound nucleus model, which is in good agreement with relative low energy experimental data, is considered. In forming a compound nucleus, an incident particle is absorbed by the nucleus, and its energy is distributed among the nucleons in a nucleus. The principal and initial assumption of the theory of the compound nucleus is satisfied only if the range of the particle in the nuclear material is considerably smaller than the dimensions of the nucleus and if the excitation energy of the compound nucleus associated with one particle is considerably smaller than the energy required to separate this particle from the nucleus. For incident particle energies greater than about 50 MeV, neither of these conditions is satisfied. Nevertheless, in the energy region up to 100 MeV, the compound nucleus model is still reasonable. It is, then, not unreasonable to consider the experimental data at high energies from the point of view of this model.

At photon energies exceeding about 60—80 MeV, the energy and momentum of the photon are also absorbed by a group of nucleons which leaves the nucleus, transferring to it only a part of the energy. One such mechanism, proposed by Levinger,[24] is the quasi-deuteron mechanism. In such an interaction, it may turn out that the probability of transferring a given portion of energy to the nucleus varies little with the energy of the incident particle and that, consequently, the cross section for the production of a given isotope will also vary little.

The reaction types leading to ^{28}Mg investigated here, *i.e.*, $(\gamma, 2\mathrm{p})$, $(\gamma, 3\mathrm{p})$, and $(\gamma, 4\mathrm{p})$, do not include the emission of neutrons. On the contrary, the reaction types leading to ^{24}Na, *i.e.*, $(\gamma, 3\mathrm{pn})$, $(\gamma, 4\mathrm{p3n})$, $(\gamma, \mathrm{d2pn})$, and others, do involve the emission of neutron. After quasi-deuteron absorption, a neutron and a proton share the energy of the incoming photon and either escape from the nucleus or collide with other nucleons. In the light nuclei region, it may be very rare that a neutron or a proton collides with other nucleus. For this reason, the reaction cross sections leading to ^{28}Mg may have small values if the cross sections depend on the quasi-deuteron process. In the energy region between 70 MeV and 150 MeV, each of the cross-section data leading to ^{28}Mg is shown to have a relatively lower value compared with the peak cross section data, but that leading to ^{24}Na has almost the same value as the peak cross section data. In the energy region between 100 MeV and 150 MeV, it is difficult to explain the

23) R. G. Korteling and A. A. Caretto, Jr., *J. Inorg. Nucl. Chem.*, **29**, 2863 (1967).

24) J. S. Levinger, *Phys. Rev.*, **84**, 43 (1951).

cross section data by the compound nucleus model, but the quasi-deutron model is suitable to explain the data.

At energies above 150 MeV, which is the pion threshold energy, the quasi-deuteron and pion production processes compete. In the case of contributions to the reaction cross section from processes associated with pion production, two types of mechanisms must be considered. One involves those events in which pions are produced and emitted from the nucleus. The other involves events in which pions are produced and then re-absorption process within the nucleus. For the light nuclei, the pion re-absorption process is generally less than 10% of that for pion emission.[22] In the energy region between 150 MeV and 250 MeV, the photo-pion reaction is the sum of the productions of both charged and neutral pions. For example, to the ^{27}Al→^{24}Na reaction is now added the following photonuclear reactions. ^{27}Al(γ, $\pi^0$2pn)^{24}Na, ^{27}Al(γ, π^+p2n)-^{24}Na, ^{27}Al(γ, π^-3p)^{24}Na, *etc.* Therefore, many reaction paths must be considered for the photon absorption processes in complex nuclei, if the pion productions take part in the reaction observed. Among the high-energy photonuclear reaction mechanisms, the quasi-deuteron and pion production processes must be considered at an initial cascade process, but the evaporation process may be considered after the cascade process. According to the cascade theory, the incident photon does not transfer all its energy to the nucleus, as is assumed in the theory of the compound nucleus, but interacts with individual nuclear particles, giving them a part of its energy. Some of the nucleons which have taken part in the cascade process fly out of the nucleus, forming the experimentally observed component of high-energy nucleons, while the rest are absorbed by the nucleus, transferring their energy to the latter. The excited nucleus thus formed after the cascade process passes back to the ground state by the evaporation process. The analytical calculation of the cascade process is, even in principle, very laborious, moreover, at the present time, it is quite impossible, since a number of the cascade characteristics have no analytical expression. Hence, in order to calculate the cascade process, the Monte Carlo statistical method may be carried out with the use of a high-speed electronic computer; such calculations will be reported elsewhere.

Recoil Study. It is very difficult to obtain information about photonuclear reaction mechanisms by velocity measurements of the protons and neutrons ejected in these complex reactions. In order to gain more information, measurements of the angular distributions of emitted particles are needed. Radiochemical techniques were suitable for observations of the recoil properties of the heavy residual nuclei. The target foils used in this experiments were 3.12 mg/cm^2 magnesium and 4.57 mg/cm^2 aluminum. These were, in all cases, considerably thicker than the fragment ranges and were surrounded by recoil catchers consisting of 3.14 mg/cm^2 Mylar foils. The fraction of the ^{24}Na atoms that recoiled from the target into the Mylar

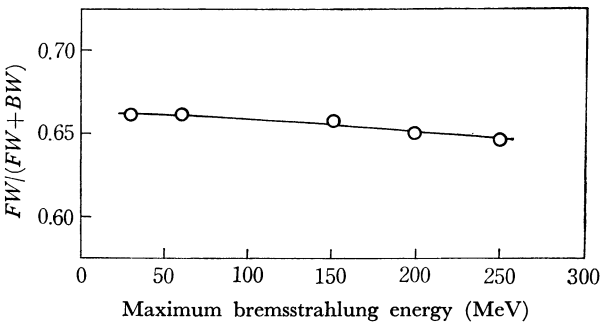

Fig. 14. Recoil fraction rate for the reaction ^{25}Mg(γ,p)^{24}Na.

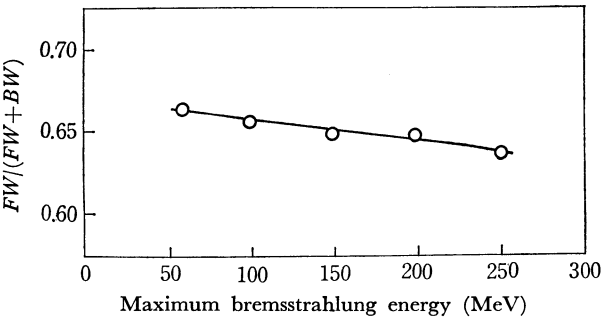

Fig. 15. Recoil fraction rate for the reaction ^{27}Al→^{24}Na.

catchers was measured by using a 3″ϕ×3″ NaI (Tl) crystal coupled with a 800-channel pulse-height analyzer. A number of thick-target recoil experiments were performed in the energy range from 30 MeV to 250 MeV. The results of the recoil studies are shown in Figs. 14 and 15. The listed quantities, FW and BW, are the fragments of the ^{24}Na atoms recoiling into the forward and backward fractions respectively. All of these data are shown in the laboratory system. It is assumed that the *FW/(FW+BW)* value shows the angular distribution of the ^{24}Na fragment. The ^{25}Mg (γ, p)^{24}Na reaction is due to the contribution from the compound nucleus process in the low-energy region.[25] Gorbunov *et al.*[13] assumed that, at energies above 60—80 MeV, the interaction of photons with nuclei proceeds mainly *via* photon absorption by a group to intranuclear nucleons. However, as may be seen in Figs. 14 and 15, in the energy range from 30 MeV to 60 MeV, the *FW/(FW+BW)* value of the ^{25}Mg(γ, p)-^{24}Na reaction is the same as that of the ^{27}Al→^{24}Na reaction. Therefore, it may be concluded that the low energy peak of the ^{27}Al→^{24}Na, ^{28}Si→^{24}Na, ^{30}Si→^{28}Mg, ^{31}P→^{24}Na, and ^{31}P→^{28}Mg reactions are due to the contribution from the compound nucleus process.

The author wishes to express his thanks to Dr. T. Kato of Tohoku University for his continuous encouragement. The crew of the Electron Linear Accelerator in the Laboratory of Nuclear Science of Tohoku University also made possible its trouble-free operation.

25) M. E. Toms and W. E. Stephens, *ibid.*, **82**, 709 (1951).